Dynamics and Statics of Nonaxisymmetric and Symmetric Liquid Bridges

J. Iwan D. Alexander, Andrew H. Resnick, William F. Kaukler and Yiqiang Zhang
Center for Microgravity and Materials Research
University of Alabama in Huntsville
Huntsville, Alabama 35899

Project summary and objectives

This program of theoretical and experimental ground-based research focuses on the understanding of the dynamics and stability limits of nonaxisymmetric and symmetric liquid bridges. There are three basic objectives: First, to determine the stability limits of nonaxisymmetric liquid bridges held between non-coaxial parallel disks, Second, to examine the dynamics of nonaxisymmetric bridges and nonaxisymmetric oscillations of initially axisymmetric bridges. The third objective is to experimentally investigate the vibration sensitivity of liquid bridges under terrestrial and low gravity conditions. Some of these experiments will require a low gravity environment and the ground-based research will culminate in a definitive flight experiment.

Motivation

The motivation for this work arises from several areas:

-Axisymmetric liquid bridge stability and dynamics have been the subject of numerous theoretical and experimental investigations, while nonaxisymmetric bridges have received less attention.

- The dynamics of liquid bridges (both axisymmetric and nonaxisymmetric), particularly the breakage of bridges and the sensitivity of bridges to vibration, are of particular importance for practical aspects of fluids handling in microgravity.

-Apart from purely fluid dynamic interests, liquid bridge stability is an important factor in determining the stability of molten liquid zones associated with floating zone crystal growth experiments, as well as model floating zone systems designed to study related thermocapillary flow phenomena.

- Finally, space experiments involving the study of zone vibration and response of liquid bridges to uncontrolled g-jitter are a suitable test of the need for vibration isolation techniques for experiments which will operate using liquid bridge configurations. Whether the bridges are melts or lower temperature liquids, the problem of rupture or breakage in response to spacecraft vibration (or g-jitter) is an important consideration for experiment design (e.g., the type of isolation, allowable zone slenderness, etc.)

Experimental Work

Experiments are conducted in a neutral-buoyancy or Plateau tank. The bridges are held between rigid supports which allow for rotation and lateral and vertical translation. Each support can be independently vibrated at frequencies less than 10 Hz. Bridge injection is automated with simultaneous recording of precise volume data. We use two imaging methods. Video images are obtained from two orthogonal cameras. In addition, a high quality Fourier transform imaging system for edge detection is being developed and the basic system assembled is now ready.

The important physical parameters are the aspect ratio of the bridge, the liquid volume and the static and dynamic Bond numbers. The liquid volume and the slenderness (aspect ratio) of the bridge depend on the precision with which lengths can be determined. The disk widths are known to within 10 μm. The length of the bridge is set by the positioning device and can be determined with a precision of 1-2 μm. Thus, for bridges of 2.5 cm length the slenderness, $\Lambda = L/2R_0$, can be determined to within ± 0.04%. Volume can be measured with a precision of 0.1 mm^3 and an accuracy of 0.1%. For the Bond number, the main error sources arise in the density and surface tension. The surface tension causes the largest error and density limits the magnitude of the smallest obtainable Bond number. The liquid bath is a methanol-water solution. Variation of the methanol concentration changes the density difference between the Dow Corning 200® silicone oil bridge and the bath. At 83% water concentration a condition of neutral buoyancy is obtained. The accuracy of our density measurements is currently 5 parts in 10^4.

Interfacial tension measurements were made using the drop weight technique [1,2]. The results are shown in Fig. 1. The interfacial tension of the silicone oil-solution interface ranges from a

low of 2.645 dyne cm^{-1} (100% methanol) to a high of 60.48 dyne cm^{-1} (100% water). We note that care must be taken in the vicinity of the neutral buoyancy point where the data diverge. This occurs because as neutral buoyancy is approached, the drop size increases exponentially, with a corresponding increase in drop-time. We extrapolated through the neutral buoyancy point using a cubic polynomial cubic fit to the data that yielded an interfacial tension at neutral buoyancy of 48.7 dyn cm^{-1}.

Experiments have been carried out in three areas.

a) Stability limits, symmetric and nonsymmetric breaking behavior of initially axisymmetric bridges.
b) Lateral shearing, squeezing and force measurements.
c) Vibration dynamics and breaking behavior.

Experimental Results

Figures 2-6 show examples of selected results for static and dynamic conditions. In all cases the images have been grabbed from video. In Figs. 2, 5 and 6, the half-illumination shows a dark background to the left of the bridge. The left side of the bridge is bright and shows a distorted view of the square background grid. The right side of the bridge is dark and its boundary contrasts with the bright background. In order to test our experimental set-up we repeated the work of Slobozhanin (see ref. [3]). In particular, we concentrated on the nonaxisymmetric loss of stability of initially axisymmetric bridges. The breaking of a static bridge is shown in Fig.2. (Note the long drawn-out neck prior to breaking and the satellite bubble that remains following the breakup). In some cases (see also Russo and Steen [4]) stability was lost to stable nonaxisymmetric rotund bridges. In other cases the bridge lost stability and broke nonaxisymmetrically (see Fig. 3.). This occurs near the transition point separating axisymmetric from nonaxisymmetric instability. The distance between the 1 cm diameter disks is 2.525 cm. Figure 4 shows shearing and squeezed-shearing configurations. Such experiments were also carried out for bridge configurations where the lower support disk was replaced by a disk attached to a cantilever arm. This allowed us to measure the interplay between the various forces applied to the lower disk.

The effects of vibration and oscillation are also being studied. Figure 5 shows laterally oscillating bridges. In Fig. 5a), the distance between the 1cm diameter disks is 2.525 cm. The upper disk moves at 1 Hz with a 0.25 cm amplitude. Figure 5b) shows a sequence with lateral motion of the upper disk with a frequency of 1 Hz and an amplitude of 0.1 cm. Note the difference in the deformation modes. Figure 6 shows a bridge oscillated laterally at 1 Hz and vertically (both disks) at 1.2 Hz. The bottom disk is rotating at 1rps. A "c-mode" is excited and interferes with an axisymmetric mode caused by the vertical oscillation.

Theory and numerical simulation

Dynamic stability of long axisymmetric bridges

A review of the literature related to liquid bridges can be found in [5]. Over the last twenty years many different studies have been carried out. Most of these papers are only concerned with static stability limits. Only a few attempts have been made to analyze the influence of the dynamics of the liquid bridge [5-12]. These efforts have been centered more in the dynamics itself than in its influence on the stability limits.

The theoretical work described is this section is part of a joint study carried out at the CMMR and at LAMF in Madrid. The study focuses on the effect of vibration on the stability limits of bridges and how vibration modifies the static stability boundaries [1]. It has been demonstrated in [7] that near the static stability limit of cylindrical liquid bridges there is a self-similar solution for the dynamics of the liquid bridge. Their analysis is based on a one-dimensional model in which the axial velocity is assumed to be dependent on the axial coordinate z and the time t, but not on the radial coordinate r . (This hypothesis is valid provided the slenderness is large enough [6]). Within the validity range of this analysis the variation with time of the interface deformation is given by Duffing's equation [14]. In addition to the Duffing equation model, we have been using the 1D-model of Zhang and Alexander [9]. Both models are in good qualitative agreement for the parameter range investigated so far. The results of the study indicate that depending on the nature of the axial vibration the bridge may be stabilized or destabilized relative to the static stability margin.

At the static stability margin the effective dimensionless potential energy ξ of the liquid bridge, which accounts for both gravity field and surface energies, in self-similar variables is

$$\xi = -\frac{1}{2}m\alpha^2 - \frac{1}{4}\alpha^4 - \beta\alpha, \tag{1}$$

where α is the amplitude of the periodic forcing, β is the effective Bond number and m is ± 1 (depending on whether the volume is greater or less than the volume of an equivalent right circular cylinder). Equilibrium shapes are given by

$$\frac{d\xi}{d\alpha} = -m\alpha - \alpha^3 - \beta = 0. \tag{2}$$

Eq. (2) has one real root if $m = +1$, which is unstable ($d^2\xi/d\alpha^2 < 0$), and three real roots, $\alpha_1 > \alpha_2 > \alpha_3$, in the case $m = -1$. The two extreme roots, α_1 and α_3, correspond to unstable equilibrium shapes. The middle one is stable. Thus, the stability margin will be the difference between the energy of the unstable equilibrium shapes and of the stable one, $\Delta\xi = \xi_{unstable} - \xi_{stable}$. This behavior is summarized in Fig. 7, The stability margin is defined by the smallest value, $\Delta\xi = \Delta\xi_1$ and is proportional to the square of the distance to the stability limit. The stability margin represents a limit to the minimum energy needed to break the liquid bridge. This means that the response of the liquid bridge will depend on the energy of the perturbation. The liquid bridge will remain stable if the energy is smaller than the corresponding stability margin and could be unstable if the energy increases. In this last case, the evolution of the liquid bridge depends on how the perturbation is imposed and on how the energy is dissipated by viscosity. Now consider the forced oscillation of the liquid bridge in gravitationless conditions ($\beta = 0$, $b \neq 0$). In that case $\alpha_2 = 0$ and $\alpha_1 = -\alpha_3 = 1$, so that $\Delta\xi = 1/4$. The time variation of the interface is

$$\alpha_{\theta\theta} + \gamma\alpha_\theta + \alpha - \alpha^3 = b\cos(\Omega\theta + \varphi), \tag{3}$$

which, assuming steady oscillations are reached, can be integrated in a first approximation [11] obtaining $\alpha = a\cos\Omega\theta$, where the amplitude a is related to viscosity, γ, and the amplitude of the perturbation, b, and to the frequency of the perturbation, Ω, through the equation

$$a^2\left(1-\Omega^2 - \frac{3}{4}a^2\right)^2 + \gamma^2\Omega^2 a^2 = b^2. \tag{4}$$

Within this approximation the oscillation of the liquid bridge is easily visualized by plotting the liquid bridge evolution in the phase space (deformation-velocity-energy diagram), as shown in Fig. 8. Note that, since we are considering an evolution, kinetic energy must be also taken into account, so that at every point of the phase space the energy will be the sum of the potential energy plus the kinetic energy:

$$\xi = \frac{1}{2}\alpha^2 - \frac{1}{4}\alpha^4 + \frac{1}{2}\alpha_\theta^2. \tag{5}$$

Two different oscillations of the liquid bridge, with amplitude $a < 1$, are shown in Fig. 8. One corresponds to $\Omega < 1$, the other to $\Omega > 1$. For the $\Omega > 1$ case, the static stability margin is exceeded ($\Delta\xi = 1/4$) but the configuration remains stable. The liquid bridge will be unstable when $a = 1$, This yields

$$\gamma^2 = \Omega^{-2}\left[b^2 - \left(\frac{1}{4} - \Omega^2\right)^2\right] \tag{6}$$

Once b and Ω are fixed, the liquid bridge evolution will be stable if the viscosity of the liquid is greater than the value resulting from (10). Otherwise it will be unstable. Results obtained by numerical integration of (3) are shown in Fig. 9. Each one of the curves b = constant represents the corresponding dynamic stability limit. Points on the right of a given curve are stable (high viscosity, γ) whereas those of the left side (low γ) are unstable. Note that, once γ and b are fixed there can be multiple values of Ω that lead to instability.

Numerical modelling of nonaxisymmetric bridges

We have developed a numerical code to deal with the vibration dynamics of axisymmetric and nonaxisymmetric bridges. For the nonaxisymmetric cases the code is currently limited because our mapping technique does not allow a full range of contact angles. The code can still be used for slender nonaxisymmetric bridges, however. The code has been checked against a previously developed axisymmetric code developed by us and against the work of Chen [15] who examined the effects of an inclined gravity vector on liquid bridge shapes. Our results for the effect of inclination angle on the minimum stable volume for fixed Bond number and aspect ratio are shown in Figs. 10-12. The results show that, for a fixed Bond number, inclining the gravity vector to the bridge axis results in a decrease in the miminum stable volume.

Summary

We have presented selected examples of our ongoing work, We have made progress in several areas especially in the area of bridge vibration dynamics and nonaxisymmetric behavior. Particularly interesting is a novel technique for measuring the changing force on one of the discs as the bridge characteristics are varied. This gives additional insight into the behavior of deforming and breaking bridges. During the next eighteen months we plan to complete a study of nonaxisymmetric breaking of axisymmetric bridges under static and dynamic conditions, a study of the static stability of bridges held between noncoaxial parallel disks and to have made significant progress into the study of vibrating bridges and the question of dynamic stability of bridges.

Acknowledgments

This work has been supported by the National Aeronautics and Space Administration through NASA grant NAG8-1384.

References

[1] M.C. Wilkinson and M.P. Aronson, Applicability of the drop-weight technique to the determination of the surface tensions of liquid metals, J. Chem. Soc., Faraday Trans., I, **69**, 474 (1973).

[2] J.M. Andreas, E.A. Hauser, and W.B. Tucker, Boundary tension by pendant drops, J. Phys. Chem., **42**, 1001 (1938)

[3] L. A. Slobozhanin and J.M. Perales, Stability of liquid bridges between equal disks in an axial gravity field, Phys. Fluids A, 5 (1993) 1305..

[4] M.J. Russo and P.H. Steen, Instability of rotund capillary bridges to general disturbances: Theory and experiment, J. Colloid Int. Sci., 113 (1986) 154.

[5] J.M. Perales, and J. Meseguer, Theoretical and experimental study of the vibration of axisymmetric viscous liquid bridges, Phys. Fluids A 4 (1992) 1110.

[6] Meseguer, J., The breaking of axisymmetric slender liquid bridges, J. Fluid Mech. 130, 123-151(1983).

[7] D. Rivas, and J. Meseguer, One dimensional, self-similar solution of the dynamics of axisymmetric slender liquid bridges, J. Fluid Mech. 138, (1984) 417.

[8] A. Sanz, J. López-Díez, Non-axisymmetric oscillations of liquid bridges, J. Fluid Mech. 205 (1989) 503.

[9] Y.Q. Zhang and J.I.D. Alexander, Sensitivity of liquid bridges to axial vibration, Physics of Fluids, A 2 (1990) 1966-1974.

[10] D. Langbein, Oscillations of finite liquid columns, Microgravity Sci. Technol. 5 (1992) 73.

[11] R.M.S.M. Schulkes, Nonlinear liquid bridge dynamics, in ESA SP-333, Vol. 1 (ESA Publ. Div., ESTEC, Noordwijk 1992) 61.

[12] J.M. Vega, and J Perales, Almost cylindrical isorotating liquid bridges for small Bond numbers, in ESA SP-191, (ESA Publ. Div., ESTEC, Noordwijk 1992), 247.

[13] J. Meseguer, M.A. Gonzalez and J.I.D. Alexander, Dynamic stability of long axisymmetric bridges, Microgravity Science and Technology, to be published.

[14] J.J. Stoker, Nonlinear vibrations, Vol. II (Interscience, 1966).

[15] H. Chen and M.Z. Saghir, Nonaxisymmetric equilibrium shapes of the liquid bridge, Microgr. Sci. Technol., 7 (1994) 12.

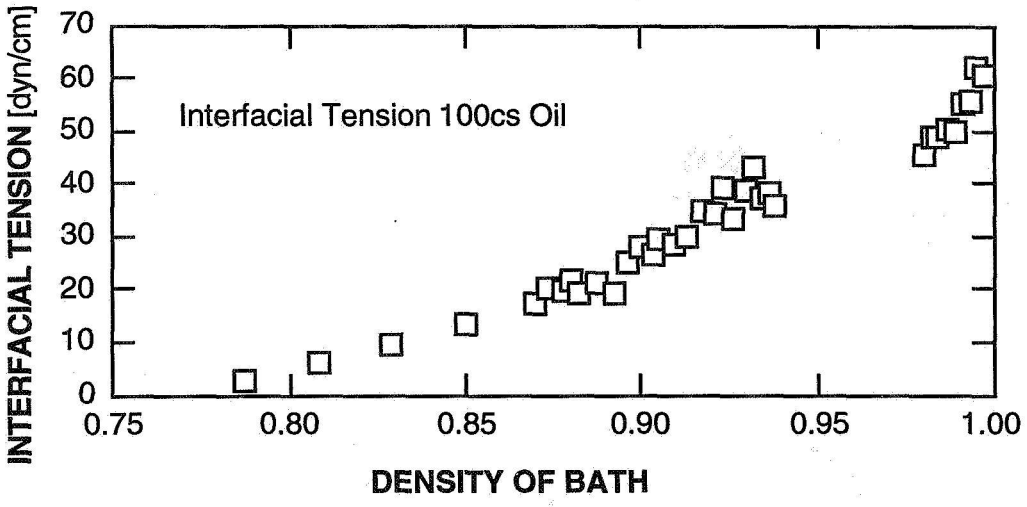

Fig. 1. Interfacial tension of Dow Corning 200 fluid-methanol/water interface as a function of methanol concentration.

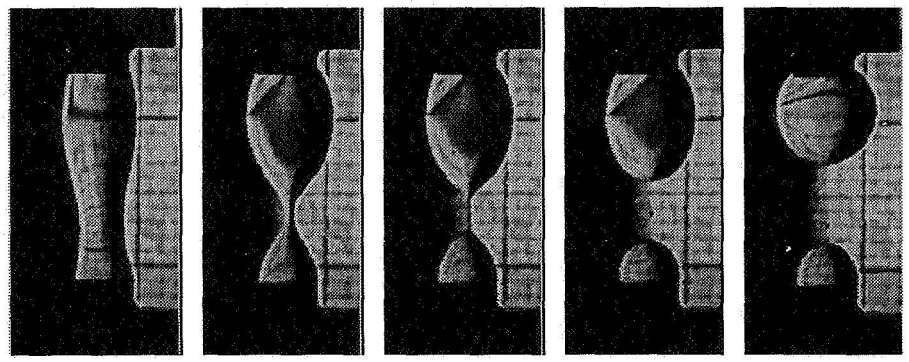

Fig. 2. Axisymmetric breaking of liquid bridge.

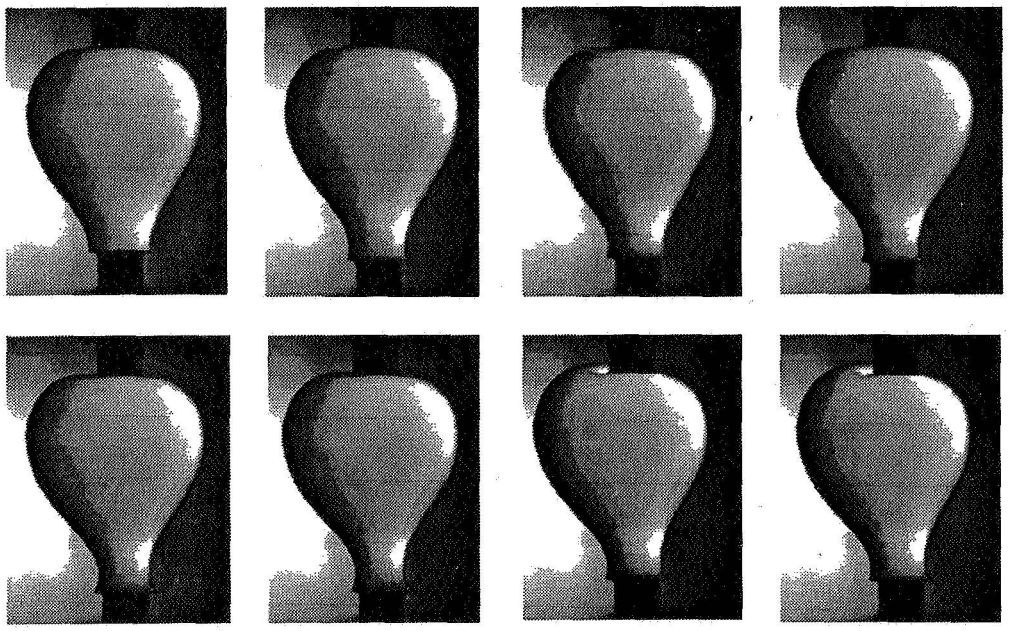

Fig. 3. Nonaxisymmetric loss of stability of an initially axisymmetric bridge. The aspect ratio and relative volume at breaking are 3.25 and 4.23, respectively. The Bond number, Bo, is 0.1.

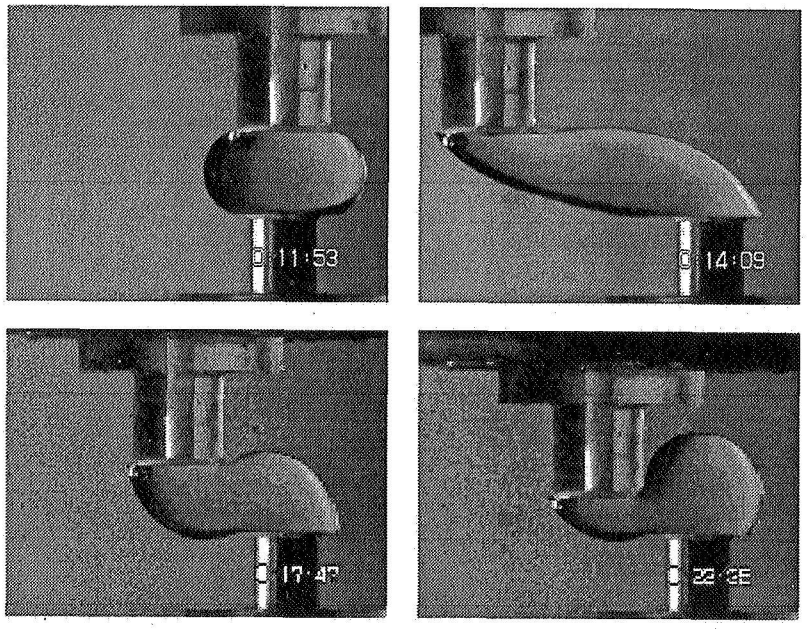

Fig. 4. Shearing and squeezing of liquid bridges.

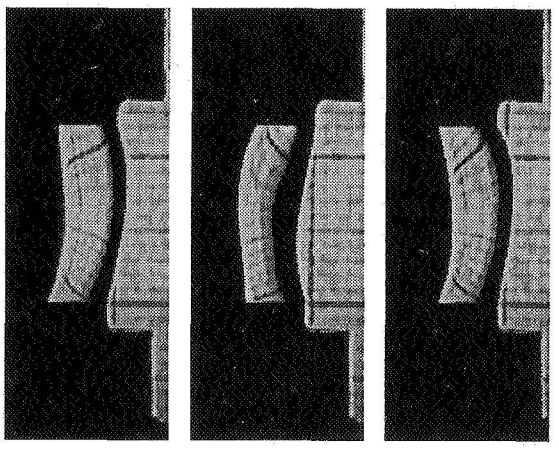

Fig 5a. Lateral oscillation at 1 Hz, 0.25 cm amplitude.

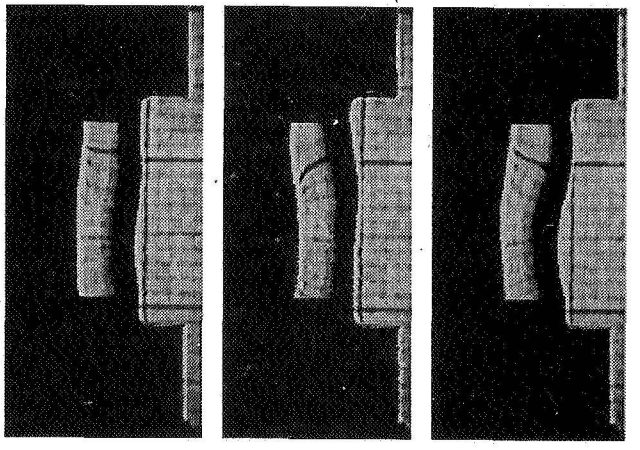

Fig. 5b. Lateral oscillation at 1 Hz, 0.1 cm amplitude.

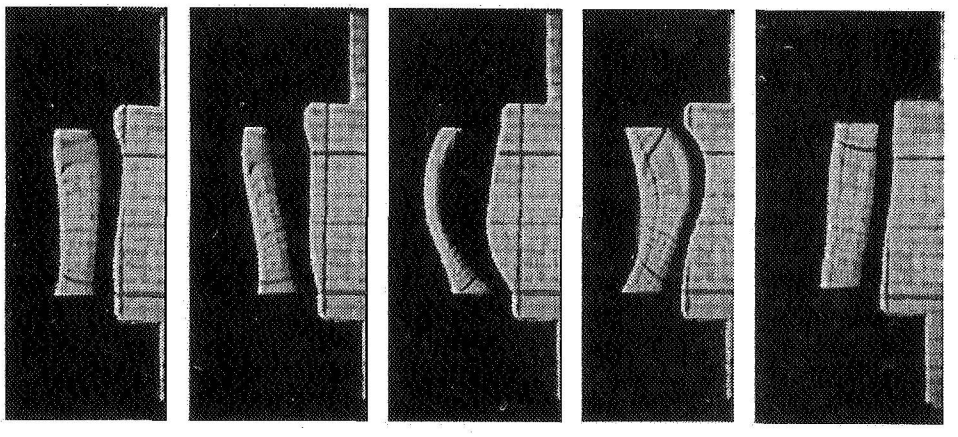

Fig. 6. Rotation (lower disk) at 1 rps, lateral oscillation (upper disk) at 1 Hz, amplitude 0.4 cm, vertical oscillation (both disks) at 1.2 Hz.

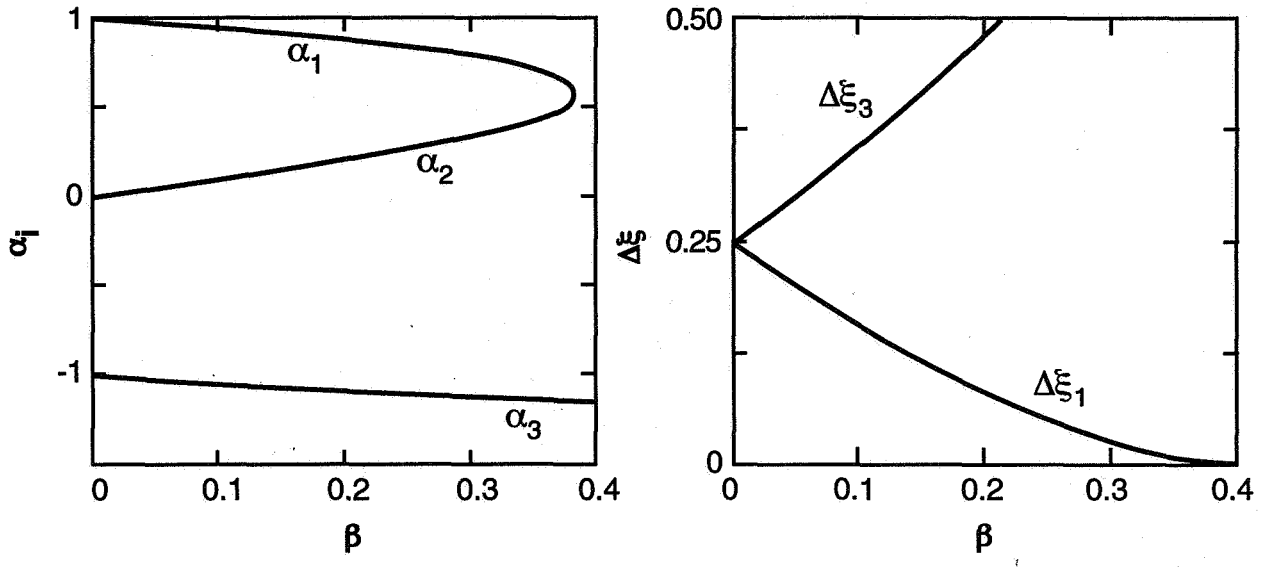

Fig. 7. Variation of the roots, α_i, (of eq. (2)) and the energy difference $\Delta\xi_i$ with the Bond number β.

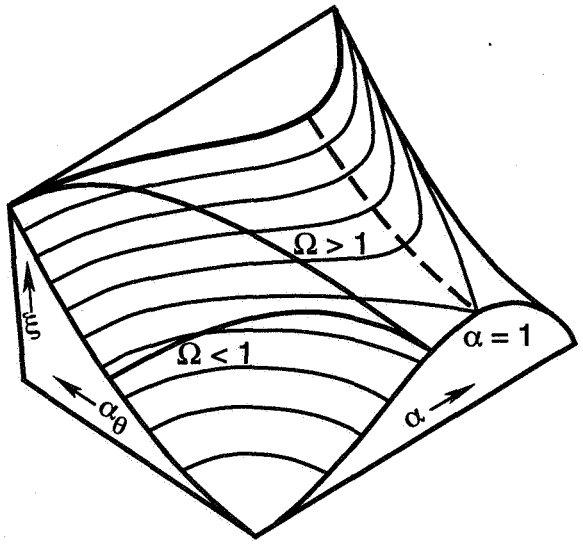

Fig. 8. Phase space of the forced oscillations of a liquid bridge according to eq. (5). Two evolutions are represented, $\Omega > 1$ and $\Omega < 1$, where Ω is the frequency of the forcing.

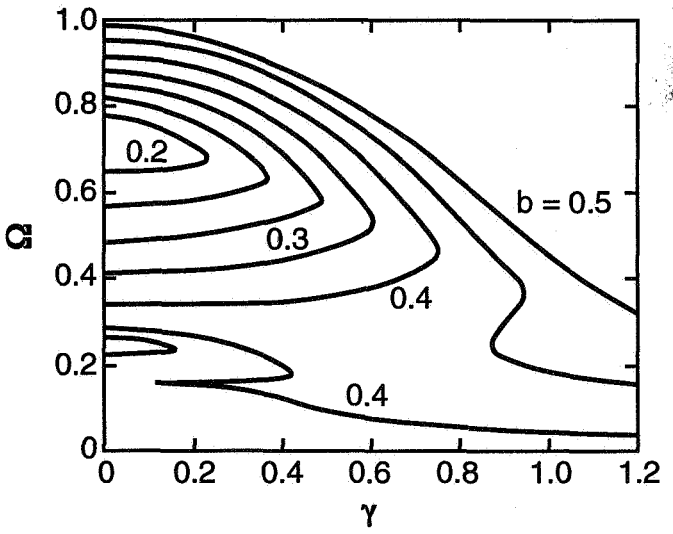

Fig. 9. Stability diagram in self-similar variables as given by eq. (6). Points on the left of each curve b = constant are unstable for this value of b, whereas those lying on the right are stable.

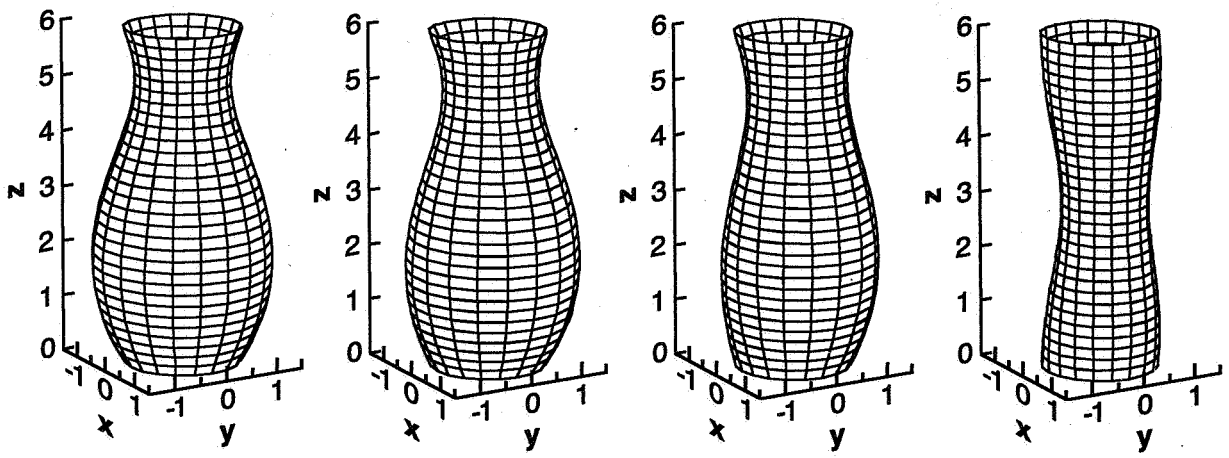

Fig. 10. Bridge profiles prior to breaking for a non-axial gravity vector. L/2r = 3, Bo = 0.05, for inclinations of a) 0, b) 30, c) 60 and d) 90 degrees, resectively.

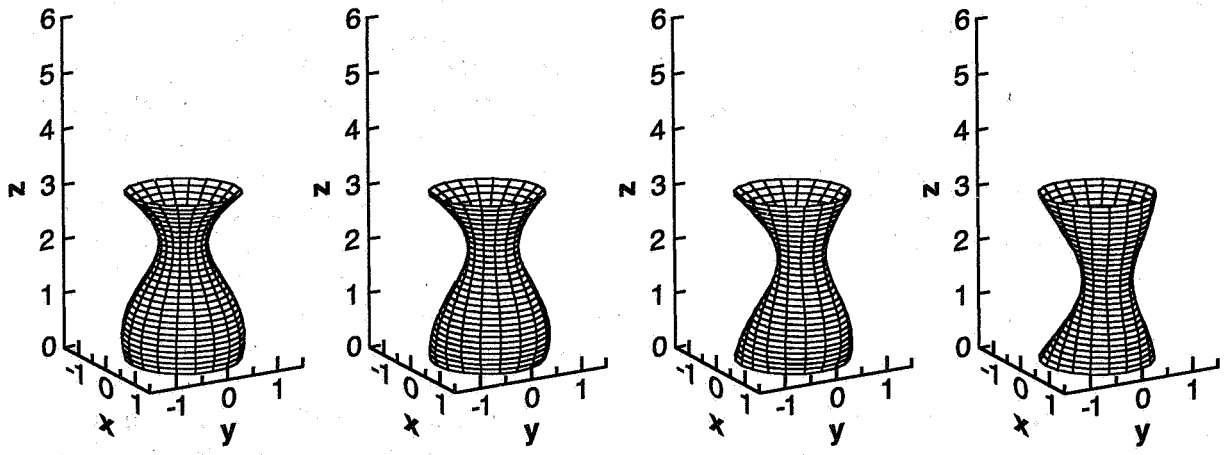

Fig. 11. Bridge profiles prior to breaking for a non-axial gravity vector. L/2r = 1.5, Bo = 0.5, for inclinations of a) 0, b) 30, c) 60 and d) 90 degrees, resectively.

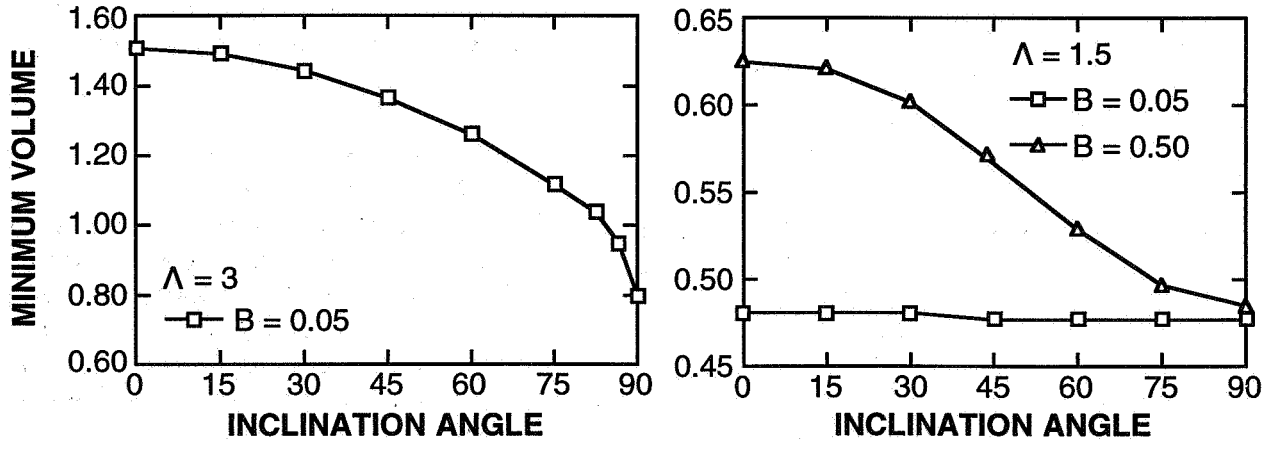

Fig. 12. Effect of inclination angle on the minimum stable volume at fixed Bo and aspect ratio.